



Cite this: *Chem. Sci.*, 2024, **15**, 1117

All publication charges for this article have been paid for by the Royal Society of Chemistry

Received 6th November 2023  
Accepted 10th December 2023

DOI: 10.1039/d3sc05946d  
[rsc.li/chemical-science](http://rsc.li/chemical-science)

## Electrochemical assembly of isoxazoles via a four-component domino reaction†

Yuanyuan Zhao,‡<sup>a</sup> Xinyue Li,‡<sup>a</sup> Simon L. Homölle, ID<sup>b</sup> Bin Wang ID<sup>a</sup> \*abc  
and Lutz Ackermann ID<sup>a,b</sup>

Multicomponent domino reactions via electrochemical annulations have emerged as a robust strategy for the rapid assembly of heterocyclics. Herein, an electrochemical annulation via a [1 + 2 + 1 + 1] four-component domino reaction was accomplished in a user-friendly undivided cell setup to assemble valuable five-membered isoxazole motifs. Our approach is characterized by a high level functional group tolerance and operational simplicity, avoiding the tedious and time-consuming preparation of pre-functionalized substrates. Detailed mechanistic studies were conducted including isotopic labeling, kinetic studies, cyclic voltammetry (CV) analysis, and intermediate characterization, providing support for a radical pathway.

## Introduction

Domino reactions<sup>1</sup> have emerged as powerful transformative strategies for the highly efficient construction of five-, six-, and seven-membered heterocycles.<sup>2</sup> Despite undeniable progress, the presence of sacrificial chemical oxidants (*e.g.*, Ag<sub>2</sub>O) and tedious operating procedures are generally indispensable in these processes. However, since the success of Kolbe electrolysis in 1847,<sup>3</sup> electricity has consistently been recognized as a green, cost-effective, and sustainable redox equivalent, and it has found widespread use in accessing desired targets, particularly in their renaissance during the last few years.<sup>4</sup> Notably, electro-organic synthesis, particularly the electrochemical annulation strategy, holds distinctive advantages such as operational simplicity and the utilization of sustainable electricity. This avenue in organic chemistry shows promise, offering abundant opportunities for the development of novel organic reaction methods, encompassing the synthesis of C–O, C–N, and C–C bonds.<sup>4f,g</sup>

Isoxazoles represent important structural motifs.<sup>5</sup> These five-membered heterocyclic compounds containing a weak N–O

bond have gained recognition as relevant building blocks in approved pharmaceutical drugs,<sup>6a</sup> bioactive molecules,<sup>6b</sup> crop protection,<sup>6c</sup> and natural products (Fig. 1).<sup>6d</sup> As such, several strategies have been developed for the successful synthesis of isoxazoles, for instance the Claisen condensation (Scheme 1a),<sup>7</sup> cyclo-isomerization (Scheme 1b),<sup>8</sup> and 1,3-dipolar cycloaddition (Scheme 1c).<sup>9</sup> These approaches have benefitted from significant contributions by the research groups of Claisen,<sup>7</sup> Willis,<sup>8</sup> Kittakoo,<sup>9a</sup> Fokin,<sup>9b</sup> and others.<sup>10</sup> However, these strategies have considerable limitations, such as the use of expensive and environmentally toxic transition metal catalysts (*e.g.* rhodium, and palladium), the requirement of pre-functionalized substrates, and having a low functional group tolerance. Recently, several innovative multicomponent strategies leading to substituted isoxazoles have been reported. These approaches involve diverse intermediates such as  $\alpha$ -alkynyl ketoximes<sup>11a</sup> and nitrostyrolenes.<sup>11b</sup> These consecutive transformations within these multicomponent systems simplify the process of creating intricate heterocyclic compounds from simple starting materials, highlighting the potential of one-pot multicomponent reactions.

Inspired by our previously successful approach for alkene cycloaddition,<sup>12</sup> we herein present a novel four-component domino reaction utilizing electricity as an environmentally friendly oxidant for the efficient assembly of valuable five-

<sup>a</sup>Key Laboratory of Xin'an Medicine of the Ministry of Education, School of Pharmacy, Anhui University of Chinese Medicine, Hefei, 230038, P. R. China. E-mail: bw5654@ahcm.edu.cn

<sup>b</sup>Institut für Organische und Biomolekulare Chemie and Wöhler Research Institute for Sustainable Chemistry (WISCh), Georg-August-Universität Göttingen, Tammannstraße 2, 37077, Göttingen, Germany. E-mail: Lutz.Ackermann@chemie.uni-goettingen.de

<sup>c</sup>Institute of Pharmaceutical Chemistry, Anhui Academy of Chinese Medicine, Hefei, 230038, P. R. China

† Electronic supplementary information (ESI) available. CCDC 2267215. For ESI and crystallographic data in CIF or other electronic format see DOI: <https://doi.org/10.1039/d3sc05946d>

‡ These authors contributed equally.

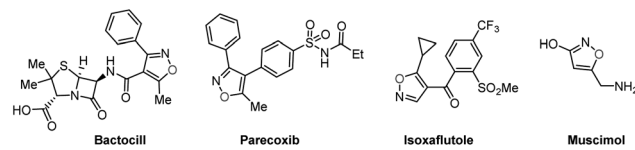
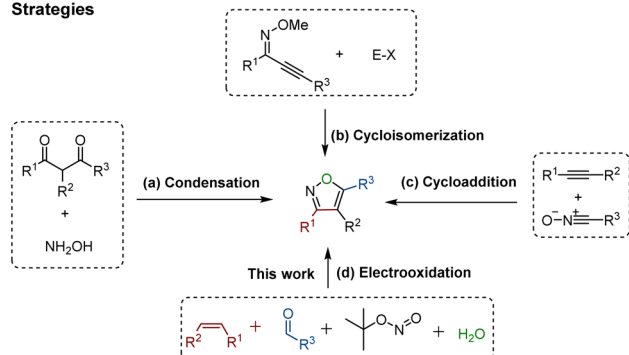


Fig. 1 Examples of bearing isoxazoles with versatile functions.



## Strategies



Scheme 1 Synthetic methods of isoxazoles.

membered isoxazole skeletons (Scheme 1d). The distinctive features of this strategy include: (a) the first electro-oxidative  $[1+2+1+1]$  cycloaddition, (b) identification and characterization of key  $\beta$ -carbonyl ketoxime intermediates, (c) use of  $\text{H}_2\text{O}$  as an unusual oxygen source, and (d) detailed mechanistic insights through isotopic labelling, kinetic investigations, CV analysis, and intermediate reactivity studies.

## Results and discussion

### Optimization of the reaction conditions

We started our studies with 4-cyanobenzaldehyde (**1a**) and styrene (**2a**), in the presence of *tert*-butyl nitrite (TBN, **3**), as model substrates, and  $\text{H}_2\text{O}$  in a user-friendly undivided cell setup using a graphite felt (GF) anode and a platinum plate (Pt) cathode (refer to Table 1 and S1 in the ESI for details). The solvent of the reaction has great influence on the yield and selectivity of the target. For instance, when employing solvents containing hydroxyl groups like hexafluoroisopropanol or *tert*-butanol, the desired product cannot be obtained. Instead, the system primarily facilitates the oxidation of the substrate, styrene, to form benzonitrile (Table S1†). The best solvent system was found to be a mixture of DMF and  $\text{H}_2\text{O}$  (2:1) (entries 1 and 2). Interestingly, LiBr as an electrolyte exhibited better electron transfer efficiency than *n*-Bu<sub>4</sub>NPF<sub>6</sub> but was, however, slightly inferior to *n*-Bu<sub>4</sub>NBr, suggesting the potential significance of the bromine anion in the synthesis (entry 3).<sup>13</sup> The introduction of acid into the reaction system proved to be advantageous for the reaction efficiency, with trifluoroacetic acid (TFA) being optimal (entry 4).<sup>14</sup> Control experiments confirmed the indispensable role of electricity while also suggesting the dual functionality of TBN as both the substrate and oxidation agent (entries 5–6). Through electrode optimization experiments, it has been demonstrated that utilizing platinum as a cathode yields superior outcomes (entry 7). Under constant current conditions, the reaction time significantly influences the formation of the desired target product **4** (entry 8 and Fig. S12, see ESI†). Broadly, the reaction progress can be categorized into three distinct stages. Initially, within the first 2 hours, the reaction system predominantly experiences an induction period, characterized by a product concentration below 0.02 M. Subsequently, spanning from 2 to 6 hours, the system enters a developmental phase, witnessing an increase in product concentration from 0.02 M to 0.155 M. Finally, beyond 6 hours, the system stabilizes into an equilibrium period. Moreover, altering the reaction temperature within certain limits did not significantly compromise the efficacy of the reaction **1a** (entry 9).

butanol, the desired product cannot be obtained. Instead, the system primarily facilitates the oxidation of the substrate, styrene, to form benzonitrile (Table S1†). The best solvent system was found to be a mixture of DMF and  $\text{H}_2\text{O}$  (2:1) (entries 1 and 2). Interestingly, LiBr as an electrolyte exhibited better electron transfer efficiency than *n*-Bu<sub>4</sub>NPF<sub>6</sub> but was, however, slightly inferior to *n*-Bu<sub>4</sub>NBr, suggesting the potential significance of the bromine anion in the synthesis (entry 3).<sup>13</sup> The introduction of acid into the reaction system proved to be advantageous for the reaction efficiency, with trifluoroacetic acid (TFA) being optimal (entry 4).<sup>14</sup> Control experiments confirmed the indispensable role of electricity while also suggesting the dual functionality of TBN as both the substrate and oxidation agent (entries 5–6). Through electrode optimization experiments, it has been demonstrated that utilizing platinum as a cathode yields superior outcomes (entry 7). Under constant current conditions, the reaction time significantly influences the formation of the desired target product **4** (entry 8 and Fig. S12, see ESI†). Broadly, the reaction progress can be categorized into three distinct stages. Initially, within the first 2 hours, the reaction system predominantly experiences an induction period, characterized by a product concentration below 0.02 M. Subsequently, spanning from 2 to 6 hours, the system enters a developmental phase, witnessing an increase in product concentration from 0.02 M to 0.155 M. Finally, beyond 6 hours, the system stabilizes into an equilibrium period. Moreover, altering the reaction temperature within certain limits did not significantly compromise the efficacy of the reaction **1a** (entry 9).

### Mechanistic studies

Several meticulously designed experiments were conducted to elucidate the potential reaction mechanism. These were subsequently monitored by nuclear magnetic resonance spectroscopy (NMR spectroscopy), High Resolution Mass Spectrometry (HR-MS), and Gas Chromatography-Mass Spectrometry (GC-MS) (for detailed information, refer to Fig. 2, S1–S8, Schemes S1 and S2 in the ESI†). Under standard conditions, isoxazole **4** was obtained with a yield of 62% (Table 1, entry 1). However, when 1.0 equivalent of 2,2,6,6-tetramethylpiperidoxyl (TEMPO) or 2,6-di-*tert*-butyl-4-methylphenol (BHT) was added to the reaction system, the yield significantly decreased, indicating that TEMPO or BHT had inhibitory effects on the formation of the desired product **4** (Fig. 2a). In addition, BHT adduct **6** (see Fig. S3†) was successfully isolated and confirmed using HR-MS, further supporting the occurrence of  $\text{N}=\text{O}$  radicals in the system. Intermolecular competition experiments involving various substituted benzaldehydes under standard conditions demonstrated that the reaction exhibited higher efficiency when using benzaldehydes containing electron-deficient substituents (Fig. 2b).

Afterwards, we conducted experiments in the presence of DMF-*d*<sub>7</sub>, D<sub>2</sub>O, and  $\text{H}_2\text{O}$ <sup>18</sup> to investigate whether solvent molecules participate in the formation of the isoxazole (refer to Fig. 2c, Schemes S1 and S2†). When employing DMF/ $\text{H}_2\text{O}$  (2:1) or DMF-*d*<sub>7</sub>/ $\text{H}_2\text{O}$  (2:1) as the solvent system, GC-MS analysis

Table 1 Optimization of the reaction conditions<sup>a</sup>

Entry	Deviation and standard conditions	Yield [ <b>4</b> ] <sup>b</sup>
1	None	62
2	CH <sub>3</sub> CN instead of DMF	21
3	<i>n</i> -Bu <sub>4</sub> NPF <sub>6</sub> /LiBr instead of <i>n</i> -Bu <sub>4</sub> NBr	25/61
4	AcOH instead of TFA	40
5	No current	8
6	CCE = 5 mA	35
7	Pt(+) I GF(–)	54
8	<i>t</i> = 4 h/10 h	38/61
9	<i>T</i> = 80 °C	52

<sup>a</sup> Reaction conditions: **1** (0.75 mmol), **2** (2.25 mmol), **3** (2.25 mmol), *n*-Bu<sub>4</sub>NBr (0.75 mmol), TFA (1.50 mmol), solvent (3.0 mL), 100 °C, 6–9 h, constant current electrolysis (CCE) at 10 mA, GF electrodes (10 mm × 10 mm × 6 mm), Pt electrodes (10 mm × 0 mm × 0.25 mm). <sup>b</sup> Yield of the isolated product, TFA = trifluoroacetic acid.



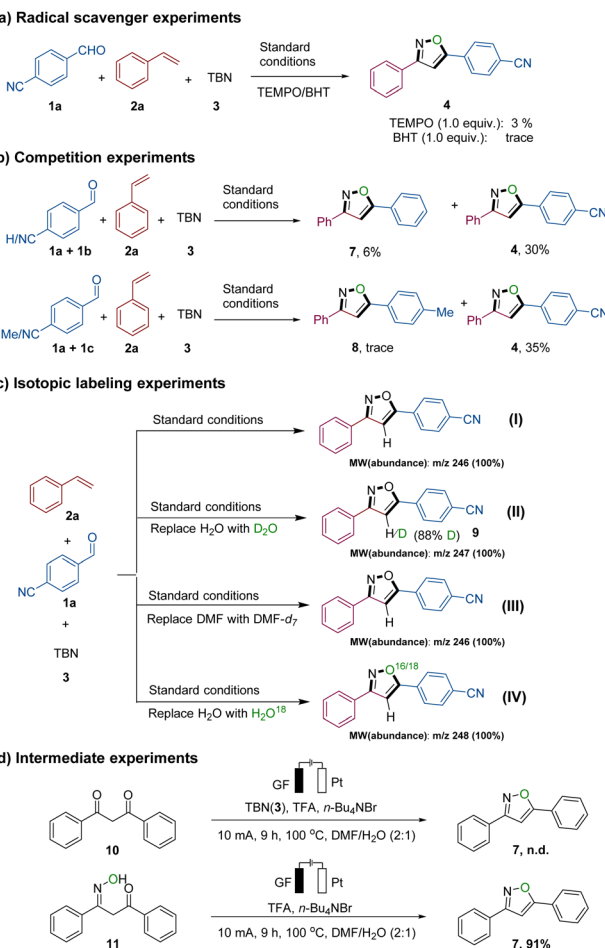


Fig. 2 Mechanistic studies: (a) the effect of radical scavengers TEMPO and BHT on the domino reaction; (b) competition reaction of **1a/1b**, and **1a/1c**, respectively, with **2a**; (c) isotope experiments: using DMF and  $\text{H}_2\text{O}$  (I), DMF and  $\text{D}_2\text{O}$  (II), DMF- $d_7$  and  $\text{H}_2\text{O}$  (III) and DMF and  $\text{H}_2\text{O}^{18}$  (IV) as solvents; (d) experiments for yielding isoxazole **7** via presumed intermediates **10** and **11**.

indicated that isoxazole **4** exhibited 100% abundance at  $m/z$  246 (isoxazole **4**, MW = 246.08). However, when DMF/ $\text{D}_2\text{O}$  (2 : 1) was used, 100% abundance was observed at  $m/z$  247. Furthermore,  $^1\text{H}$  NMR results indicated that the deuteration ratio of the hydrogen atom at position 4 of the isoxazole **4** skeleton was 88% (see NMR analysis in Fig. S4 $\dagger$ ). Notably, when  $\text{H}_2\text{O}$  was replaced with  $\text{H}_2\text{O}^{18}$ , GC-MS analysis showed an unexpected 100% abundance at  $m/z$  248. This observation may be attributed to the interaction of TBN with water molecules, resulting in the *in situ* generation of a new N=O species (IV). Subsequently, the oxygen atom from the water was successfully incorporated into the isoxazole molecule. Therefore, based on our observations, there are two main sources of nitric oxide species involved in isoxazole generation: Pathway one involves the release of N=O species (III) from TBN, while pathway two entails the interaction of TBN with water to produce the molecule  $\text{HNO}_2$ , which further generates the N=O species (IV). These findings imply that (a) the solvent water actively participates in the formation of the isoxazole, (b) the hydrogen atom at position 4 of the isoxazole **4**

skeleton partly originates from the  $\text{H}_2\text{O}$  molecule, and (c) the oxygen atom of the isoxazole skeleton is derived not only from TBN but also from  $\text{H}_2\text{O}$  (Scheme S2 $\dagger$ ).

Drawing upon our previous discoveries and relevant reports, $^{7b,12b,15}$  we introduced two presumed intermediates, **10** and **11**, individually into the reaction (Fig. 2d). When we changed the mixture of **1a** and **2a** to 1,3-dicarbonyl compound **10**, the isoxazole **4** was not detected. However, when **11** was used as a substrate, the product **4** was formed in excellent yield (91%). This leads us to believe that compound **11** is a plausible intermediate in the generation of **4**. Moreover, kinetic studies (refer to Fig. S6–S8 $\dagger$ ) indicated that the reaction exhibited a first-order dependence on the concentration of alkene **2** as well as TBN (3), while a zero-order dependence on the concentration of aldehyde **1** was observed. These findings strongly suggest that in the rate-limiting step of the transformation solely alkene **2** and TBN (3) are involved.

Subsequently, we conducted cyclic voltammetry studies to assess the oxidative electrochemical transformation (see Fig. 3). Substrates **1a** and **3** exhibited irreversible oxidation peaks at 0.99 and 1.13 V vs. saturated calomel electrode (SCE), respectively. Substrate **2a** did not exhibit an obvious oxidation peak between the potential window used. Interestingly, when a mixture of substrates **1a**, **2a**, and **3** was used, the oxidation potential of **1a** was shifted to 0.73 V vs. SCE, indicating crucial anodic oxidation of the substrate. Additionally, irreversible oxidation of product **4** was observed at potentials beyond 1.25 V vs. SCE, ensuring that the isoxazole-formation can be carried out under shown mild constant-potential electrocatalysis.

Based on the aforementioned findings and existing reports, $^{16}$  we propose a plausible reaction mechanism, which is depicted in Scheme 2. Initially, bromine anions from the electrolyte undergo oxidation at the anode, $^{13}$  leading to the formation of bromine radical **I**. Simultaneously, under thermal conditions, TBN undergoes homolysis, generating radicals **II** and **III**. $^{15}$  The reaction commences with the formation of acyl radical **A**, which is generated *in situ* through the reaction of aldehyde **1** with radical **I** or **II**. Subsequently, radical **A** attacks the double bond

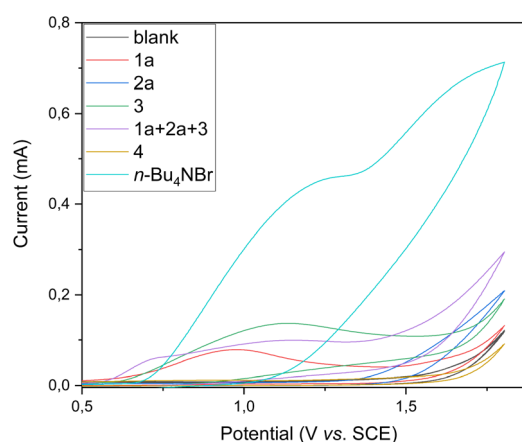
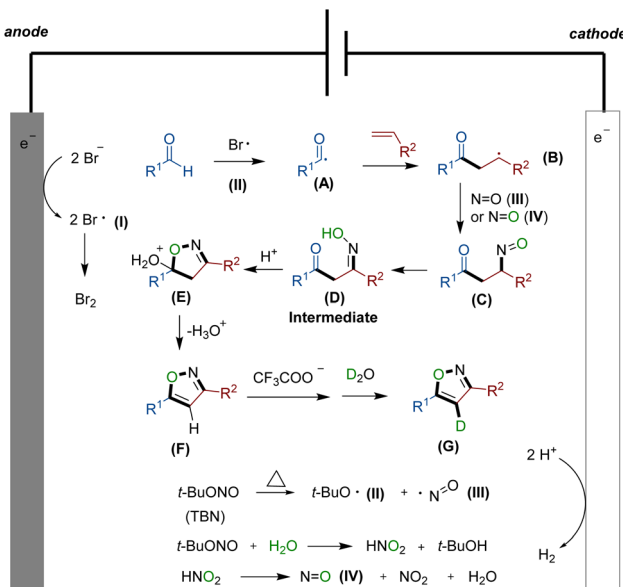


Fig. 3 Cyclic voltammetry studies at  $100\text{ mV s}^{-1}$  in DMF/ $\text{H}_2\text{O}$  (2 : 1) using tetrabutylammonium hexafluorophosphate (TBAPF<sub>6</sub>, 100 mM) as the electrolyte.



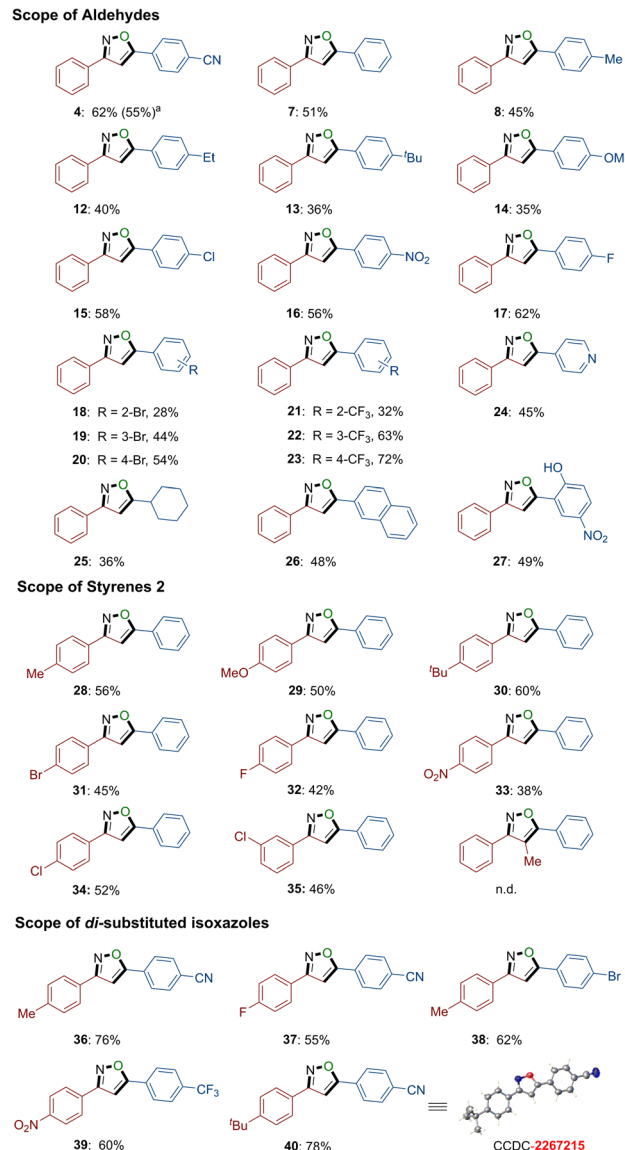


Scheme 2 Plausible reaction mechanism.

of alkene, forming a carbon-central radical **B**. Concurrently, with the assistance of N=O radical **III** or **IV**, compound **C** is generated. This is then followed by an isomerization process, rapidly yielding the crucial intermediate  $\beta$ -carbonyl ketoxime **D**. The addition of TFA promotes the dehydration of intermediate **D** facilitating the formation of the desired isoxazole **F** from **E**. Simultaneously, **F** has the potential to undergo hydrogen loss at site 4 of the isoxazole skeleton when influenced by a carboxylic acid anion. Subsequently, it can abstract a proton from deuterated water molecules to obtain deuterium-substituted moiety **G**.

### Substrate scope

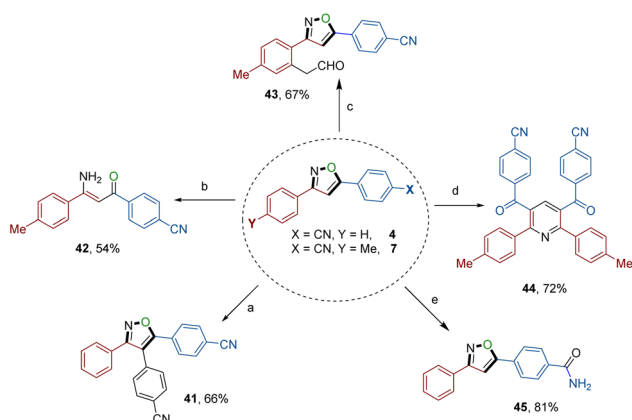
With the optimized experimental conditions in hand, we proceeded to explore the viable substrate scope of the four-component domino reaction using variously substituted aldehydes **1** (refer to Scheme 3). The reaction demonstrated high efficacy in the selective electrochemical alkene annulations, accommodating aldehydes bearing both electron-donating and electron-withdrawing groups (4, 7–8, 12–27). A wide range of functional groups, including cyano (4), alkyl (8, 12–13), ether (14), chloro (15), nitryl (16), fluoro (17), bromo (18–20), trifluoromethyl (21–23), and hydroxy (27), were well tolerated within the four-component domino reaction. Notably, even challenging substrates such as heterocyclic substrate 4-formyl pyridine, aliphatic substrate cyclohexane carboxaldehyde, and condensed ring substrate 2-naphthaldehyde could be efficiently transformed into the desired products 24, 25, and 26, respectively, with moderate to good yields. Subsequently, the scope was further extended to various tethered styrene substrates (refer to Scheme 3). Styrenes bearing *tert*-butyl (30), nitryl (33), and chloro (34) substituents effectively furnished the desired products with good yields. Furthermore, various functional groups, including alkyl (28), ether (29), bromo (31), and fluoro



Scheme 3 Electrochemical synthesis of isoxazoles via a four-component domino reaction. Reaction conditions: **1** (0.75 mmol), **2** (2.25 mmol), **3** (2.25 mmol), *n*-Bu<sub>4</sub>NBr (0.75 mmol), TFA (1.50 mmol), DMF/H<sub>2</sub>O (2 : 1, 3.0 mL), 100 °C, 6–9 h, CCE @ 10 mA, GF electrodes (10 mm × 10 mm × 6 mm), Pt electrodes (10 mm × 10 mm × 0.25 mm). Yield of the isolated product. <sup>a</sup>Gram-scale synthesis.

(32), were also well tolerated in the electrochemical annulation system. The unexpectedly relatively lower yields can be attributed to the fact that the substrate styrene may undergo conversion to both the corresponding major product, isoxazole, and the by-product 5, as evidenced by the results of electrochemical annulation and previous findings.<sup>17</sup> Notably, when  $\alpha$ -methyl styrene was used as a substrate, no desired product was observed, revealing that steric effects are significantly important in this transformation. Remarkably, the electrochemical annulation system exhibited excellent functional group tolerance, enabling the facile assembly of di-substituted isoxazole products, namely **36–40**. Moreover, the configuration of product **40** was further confirmed by X-ray crystal diffraction (Scheme 3 and





**Scheme 4** Late-stage diversification to access 3,4,5-trisubstituted isoxazole 41, aminoketone 42, and isoxazoles possessing formyl (43), phenyl pyridine (44), and amide (45) groups. (For detailed information, see the ESI†).

ESI†). In our protocol, the electronic properties of the substrate play a crucial role in product formation. For instance, employing electron-rich benzaldehyde substrates and electron-deficient olefin substrates often results in yields below 40%. Additionally, ortho-substituted substrates typically yield only moderate yields, underscoring the substantial impact of steric effects in this transformation. Conversely, choosing an electron-deficient benzaldehyde and an electron-rich olefin substrate with reduced steric hindrance can enhance the efficiency of this reaction.

#### Late-stage diversification

The exceptional synthetic applicability of the electrochemical annulation approach was further extended to late-stage diversification (Scheme 4), leading to the formation of synthetically valuable building blocks and biologically significant motifs. Treating isoxazole 4 with 4-bromobenzonitrile in the presence of a palladium chloride catalyst resulted in the formation of a particularly noteworthy 3,4,5-trisubstituted isoxazole 41.<sup>18</sup> Additionally, isoxazole 4 underwent reaction with hydrogen peroxide, generating a drug-like compound containing an amide group (45). Furthermore, the N–O bond within the isoxazole skeleton was utilized as a synthon and successfully cleaved using a copper catalyst, yielding a drug-like molecule, the  $\beta$ -aminoketone derivative (42).<sup>19</sup> Moreover, product isoxazole 7 served as a versatile precursor of two synthetically useful isoxazoles: one possessing a formyl group (43) and another a phenyl pyridine derivative (44).<sup>20</sup> These transformations were achieved through a ruthenium-catalyzed coupling reaction involving vinylene carbonate and a copper-catalyzed cyclization reaction involving dimethylsulfoxide (DMSO), respectively.

#### Conclusion

In conclusion, we have introduced an innovative electrochemical annulation strategy for the cost-effective assembly of

3,5-di-substituted isoxazoles, which can be successfully accomplished by harnessing readily available substrates. The exceptional versatility of this approach is underscored by its capacity for late-stage diversification, exemplified through the synthesis of drug-like molecules and valuable synthons such as aminoketones, phenyl pyridines, amides, and 3,4,5-trisubstituted isoxazoles. This four-component domino reaction stands as a powerful and adaptable route for the construction of isoxazoles, showcasing significant potential for the creation of diverse heterocyclic compounds. Applications of this four-component domino reaction hold promising implications in drug discovery and materials science domains.

#### Data availability

All experimental data, procedures for data analysis, and pertinent data sets are provided in the ESI.†

#### Author contributions

Y. Z and Y. L. conducted the experiments; Y. Z did the CCDC; S. L. H. carried out the cyclic voltammetry studies; B. W. and L. A. conceived the project; B. W. and L. A. wrote, reviewed, and edited the manuscript; All authors discussed the results.

#### Conflicts of interest

There are no conflicts to declare.

#### Acknowledgements

We are grateful to the support from the Overseas Study Project (gxgwx2020039), the Natural Science Foundation of Anhui province (2008085MH271), the ERC Advanced Grant (101021358) and the DFG Gottfried Wilhelm Leibniz award (L. A.).

#### Notes and references

- 1 L. F. Tietze, *Chem. Rev.*, 1996, **96**, 115–136.
- 2 (a) Y. Liu, D. Ni, B. G. Stevenson, V. Tripathy, S. E. Braley, K. Raghavachari, J. R. Swierk and M. K. Brown, *Angew. Chem., Int. Ed.*, 2022, **61**, e202200725; (b) D. M. Flores, M. L. Neville and V. A. Schmidt, *Nat. Commun.*, 2022, **13**, 2764; (c) T. Fujii, S. Gallarati, C. Corminboeuf, Q. Wang and J. Zhu, *J. Am. Chem. Soc.*, 2022, **144**, 8920–8926; (d) X. Abel-Snape, G. Wycich and M. Lautens, *ACS Catal.*, 2022, **12**, 3291–3301; (e) J. Gong, Q. Wang and J. Zhu, *Angew. Chem., Int. Ed.*, 2022, **61**, e202211470; (f) Y. Wang, J. C. A. Oliveira, Z. Lin and L. Ackermann, *Angew. Chem., Int. Ed.*, 2021, **60**, 6419–6424.
- 3 M. Yan, Y. Kawamata and P. S. Baran, *Chem. Rev.*, 2017, **117**, 13230–13319.
- 4 (a) T. Münchow, S. Dana, Y. Xu, B. Yuan and L. Ackermann, *Science*, 2023, **379**, 1036–1042; (b) S. Ji, L. Zhao, B. Miao, M. Xue, T. Pan, Z. Shao, X. Zhou, A. Fu and Y. Zhang, *Angew. Chem., Int. Ed.*, 2023, **62**, e202304434; (c) S. L. Homölle, M. Stangier, E. Reyes and L. Ackermann,



*Precis. Chem.*, 2023, **1**, 382–387; (d) L. F. T. Novaes, J. Liu, Y. Shen, L. Lu, J. M. Meinhardt and S. Lin, *Chem. Soc. Rev.*, 2021, **50**, 7941–8002; (e) L. Ackermann, *Acc. Chem. Res.*, 2020, **53**, 84–104; (f) T. Ali, H. Wang, W. Iqbal, T. Bashir, R. Shah and Y. Hu, *Adv. Sci.*, 2023, **10**, 2205077; (g) Y. A. Wu, R. A. Wang, S. Y. Jiang, T. B. Jiang, J. R. Song, J. Shi, W. Wu, W. D. Pan and H. Ren, *Green Chem.*, 2022, **24**, 6720–6726.

5 (a) C. P. Pandhurnekar, H. C. Pandhurnekar, A. J. Mungole, S. S. Butoliya and B. G. Yadao, *J. Heterocycl. Chem.*, 2023, **60**, 537–565; (b) F. Hu and M. Szostak, *Adv. Synth. Catal.*, 2015, **357**, 2583–2614.

6 (a) G. C. Arya, K. Kaur and V. Jaitak, *Eur. J. Med. Chem.*, 2021, **221**, 113511; (b) B. Heasley, *Angew. Chem., Int. Ed.*, 2011, **50**, 8474–8477; (c) X. L. Sun, Z. M. Ji, S. P. Wei and Z. Q. Ji, *J. Agric. Food Chem.*, 2020, **68**, 15107–15114; (d) J. Li, Z. Lin, W. Wu and H. Jiang, *Org. Chem. Front.*, 2020, **7**, 2325–2348.

7 (a) R. Harigae, K. Moriyama and H. Togo, *J. Org. Chem.*, 2014, **79**, 2049–2058; (b) L. Claisen and O. E. Lowman, *Ber. Dtsch. Chem. Ges.*, 1888, **21**, 1149–1157.

8 (a) F. Zhou, C. Li, M. Li, Y. Jin, H. Jiang, Y. Zhang and W. Wu, *Chem. Commun.*, 2021, **57**, 4799–4802; (b) M. Hu, Z. Lin, J. Li, W. Wu and H. Jiang, *Green Chem.*, 2020, **22**, 5584–5588; (c) R. N. Straker, M. K. Majhail and M. C. Willis, *Chem. Sci.*, 2017, **8**, 7963–7968; (d) K. N. Tu, J. J. Hirner and S. A. Blum, *Org. Lett.*, 2016, **18**, 480–483.

9 (a) C. Kesornpun, T. Aree, C. Mahidol, S. Ruchirawat and P. Kittakoop, *Angew. Chem., Int. Ed.*, 2016, **55**, 3997–4001; (b) S. Grecian and V. V. Fokin, *Angew. Chem., Int. Ed.*, 2008, **47**, 8285–8287.

10 (a) W. Wu, Q. Chen, Y. Tian, Y. Xu, Y. Huang, Y. You and Z. Weng, *Org. Chem. Front.*, 2020, **7**, 1878–1883; (b) W. Wei, Y. Tang, Y. Zhou, G. Deng, Z. Liu, J. Wu, Y. Li, J. Zhang and S. Xu, *Org. Lett.*, 2018, **20**, 6559–6563; (c) P. A. Allegretti and E. M. Ferreira, *Chem. Sci.*, 2013, **4**, 1053–1058; (d) D. Roy, S. Mom, S. Royer, D. Lucas, J. C. Hierso and H. Doucet, *ACS Catal.*, 2012, **2**, 1033–1041; (e) J. A. Burkhard, B. H. Tchitchanov and E. M. Carreira, *Angew. Chem., Int. Ed.*, 2011, **50**, 5379–5382; (f) F. Gasparini, M. Giovannoli, D. Misiti, G. Natile, G. Palmieri and L. Maresca, *J. Am. Chem. Soc.*, 1993, **115**, 4401–4402.

11 (a) X. W. Zhang, W. L. Hu, S. Chen and X. G. Hu, *Org. Lett.*, 2018, **20**, 860–863; (b) M. Fu, H. Li, M. Su, Z. Cao, Y. Liu, Q. Liu and C. Guo, *Adv. Synth. Catal.*, 2019, **361**, 3420–3429.

12 (a) J. Loup, V. Müller, D. Ghorai and L. Ackermann, *Angew. Chem., Int. Ed.*, 2019, **58**, 1749–1753; (b) L. Chen, Z. Wang, H. Liu, X. Li and B. Wang, *Chem. Commun.*, 2022, **58**, 9152–9155; (c) H. Wang, N. Kaplaneris and L. Ackermann, *Cell Rep. Phys. Sci.*, 2020, **1**, 100178.

13 (a) L. G. Gombos and S. R. Waldvogel, *Sustainable Chem.*, 2022, **3**, 430–454; (b) Z. X. Luo, M. Liu, T. Li, D. C. Xiong and X. S. Ye, *Front. Chem.*, 2021, **9**, 796690.

14 E. Trogu, C. Vinattieri, F. D. Sarlo and F. Machetti, *Chem. – Eur. J.*, 2012, **18**, 2081–2093.

15 (a) B. Wang, Z. Yan, L. Liu, J. Wang, Z. Zha and Z. Wang, *Green Chem.*, 2019, **21**, 205–212; (b) Y. Liu, J. L. Zhang, R. J. Song, P. C. Qian and J. H. Li, *Angew. Chem., Int. Ed.*, 2014, **53**, 9017–9020.

16 B. Wang, L. Tang, L. Liu, Y. Li, Y. Yang and Z. Wang, *Green Chem.*, 2017, **19**, 5794–5799.

17 U. Dutta, D. W. Lupton and D. Maiti, *Org. Lett.*, 2016, **18**, 860–863.

18 S. U. Dighe, S. Mukhopadhyay, S. Kolle, S. Kanojiya and S. Batra, *Angew. Chem., Int. Ed.*, 2015, **54**, 10926–10930.

19 C. Wan, J. Pang, W. Jiang, X. W. Zhang and X. G. Hu, *J. Org. Chem.*, 2021, **86**, 4557–4566.

20 J. Li, K. Korvorapun, S. D. Sarkar, T. Rogge, D. J. Burns, S. Warratz and L. Ackermann, *Nat. Commun.*, 2017, **8**, 15430.

